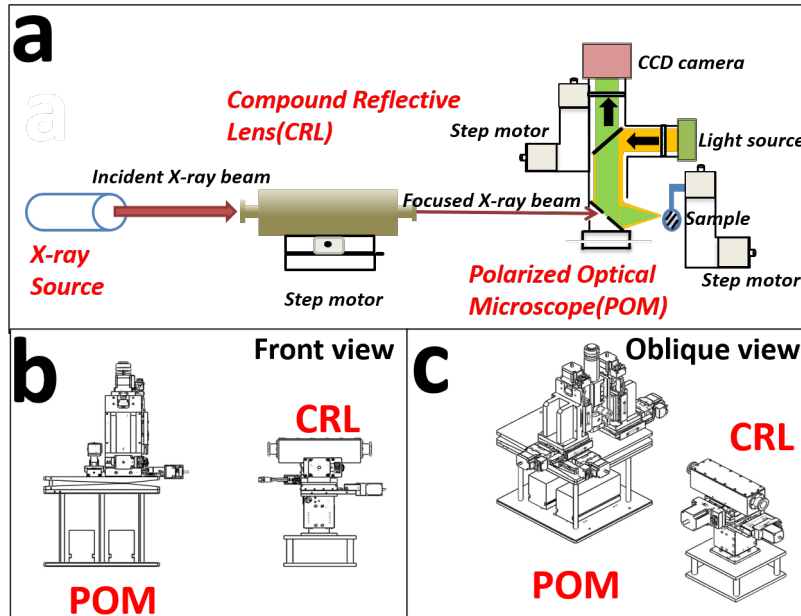


# Contents

<b>1</b>	<b>Introduction</b>	<b>1</b>
<b>2</b>	<b>Experiment</b>	<b>4</b>
2.1	Construction of stable light path . . . . .	4
2.1.1	CRL parameter determination . . . . .	4
2.1.2	Reduce beam jitter . . . . .	7
2.2	Construction of the combined system . . . . .	7
2.3	Determination of spot parameters . . . . .	9
2.4	Collection of micro-focus X-ray scattering data . . . . .	10
<b>3</b>	<b>Application</b>	<b>11</b>
3.1	Microstructure of ringed spherulites . . . . .	12
3.2	The skin and core structure of the fiber . . . . .	14
<b>4</b>	<b>Conclusion</b>	<b>14</b>

## 1 Introduction

Macromolecules are characterized by their long-chain structure, including molecular chain unit and conformation on angstrom scale, lamella on nanometer scale and spherulites on micron scale. Nowadays, synchrotron radiation small angle X-ray scattering (SAXS) and wide angle X-ray diffraction (WAXD), as a non-destructive, highly statistically averaged structure analysis method, have been widely used in crystalline polymer research area. For instance, study information on grains in crystalline polymer, micro-domains in blended polymers and the shape, size and distribution of cavities and cracks can be obtained by guinier scattering. Study information on orientation, thickness and crystalline fraction of crystalline layer and the thickness of amorphous layer of the lamella can be obtained by long-period measurement.



**Fig. 1.** Whole system

10 In order to further study the internal structure of polymers, two new test condition are required. Firstly,  
 11 considering the size of polymer spherulites, an X-ray spot with a size of  $5\mu m \cdot 5\mu m$  is needed. A small spot  
 12 provides sufficient spatial resolution when the structure of macromolecules are characterized by the SAXS  
 13 method. Secondly, In order to match the detection result with the real structure, confirming the real-time  
 14 exact position of X-ray incident beam on polymer crystal is a critical measure.

15 To improve the spatial resolution of synchrotron radiation experiment, the world's advanced synchrotron  
 16 radiation light sources all use micro-focusing to focus the spot to the micron or even sub-micron level.  
 17 Representative beamline stations include DSEY-PETRA III P03, SSRF BL15U1. However, limited by the  
 18 distance between the sample and the detector, SAXS experiment can not be implemented on these stations.

19 The main components used for X-ray beam focusing are Kirkpatrick-Baez mirror, Fresnel zone plates,  
 20 Capillary optical lens and Compound refractive lenses. In synchrotron radiation area, Kirkpatrick-Baez  
 21 mirror(K-B mirror) and Compound refractive lenses(CRLs) are more widely used. The advantages of K-B

22 mirror are aberration-free imaging on both horizontal and vertical planes, no dispersion, high energy, high  
23 reflectivity and low flux loss. However, there are some disadvantages which should be considered. K-B  
24 mirror micro-beam focusing needs to be achieved by adjusting the K-B two mirrors and multi-axis spatial  
25 attitude, including: the angle at which X-rays are incident on the mirrors, the vertical angle of the two  
26 mirrors, spatial parallelism of two vertical cylinders. The deployment of K-B mirror changes the original  
27 optical path. As a result, this off-axis device increases the complexity of installation of itself and other  
28 experimental equipment. This is unfavorable for the entire micro-focusing experiment process.

29 Compound refractive lenses(CRL) are composed of a series of single lenses arranged in a linear array  
30 to achieve X-ray focusing in the energy range of 5-40 keV. As shown in [Fig. 2](#), the most widely used CRL  
31 are parabolic compound refraction lenses. The parabolic CRL has a parabolic surface that rotates around  
32 the axis of symmetry to form a parabola. It can focus X-rays in two dimensions without causing aberrations  
33 in theory. Compared to K-B mirror, CRL does not change the original optical path propagation direction,  
34 has good high temperature stability and easy cooling, simple and compact structure, easy to adjust, low  
35 requirements for lens' surface roughness, relatively insensitive to vibration and many other advantages.  
36 The disadvantage of CRL is the low transmission efficiency. Because the aperture of the diaphragm is small  
37 and the X-rays are absorbed when they penetrate the lens' material, the focused light intensity will drop by  
38 one to two orders of magnitude. Despite this, the luminous flux can be maintained at  $10^{10} \sim 10^{11}$  phs/s after  
39 using CRL to focus the spot. This flux is enough to study the structure of crystalline polymers.

40 Polarized optical microscopy(POM) is widely used for studying polymer crystal morphology. POM is  
41 a simple method to distinguish the change of growth direction of crystals in the film plane and to check  
42 whether there exists twisting of crystals[[1](#)]. [Fig. 3](#) is a schematic diagram of the disassembly of a POM.  
43 When the polarized light generated by the polarizer and the analyzer enters the anisotropic polymer crys-  
44 tal, birefringence occurs, and the crystal contrast is obtained through the coherence of the polarized light.  
45 Different crystal forms of polymers, such as spherulites, string crystals, stretched chain crystals, transverse  
46 crystals, etc., all have anisotropic optical properties, so their crystal morphology, size, number, etc. can be

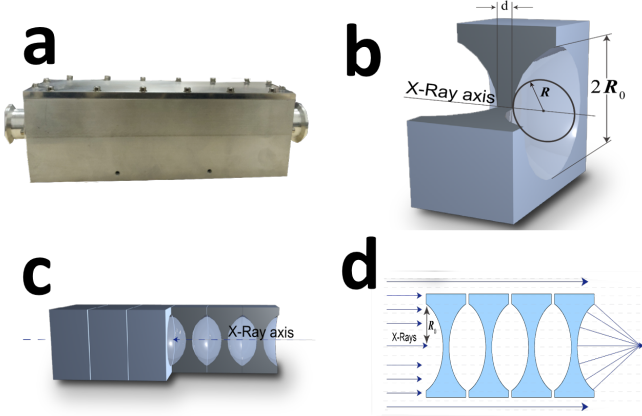


**Fig. 2.** Structure of Compound reflective lenses

47 observed with a POM.

48 In this passage, a combined device of micro-focus synchrotron radiation small-angle scattering and po-  
 49 larizing microscope is proposed. A series of parameters of the device are adjusted, and the device is used to  
 50 characterize the crystalline morphology and microstructure of related polymers.

## 51 **2 Experiment**

### 52 **2.1 Construction of stable light path**

#### 53 **2.1.1 CRL parameter determination**

54 In order to obtain the designed X-ray microbeam, CRL's parameters need to be determined first. The param-  
 55 eter mainly include material, geometric size and number of pieces. Commonly used CRL is aluminum and  
 56 beryllium. According to the theory of atomic physics, materials with low atomic number have less absorp-  
 57 tion of X-rays. In this system, a beryllium CRL is chosen because the X-ray energy needs to be preserved  
 58 as much as possible.

59 There are three common single mirrors. The main geometric parameters of them are listed in [Table 1](#).

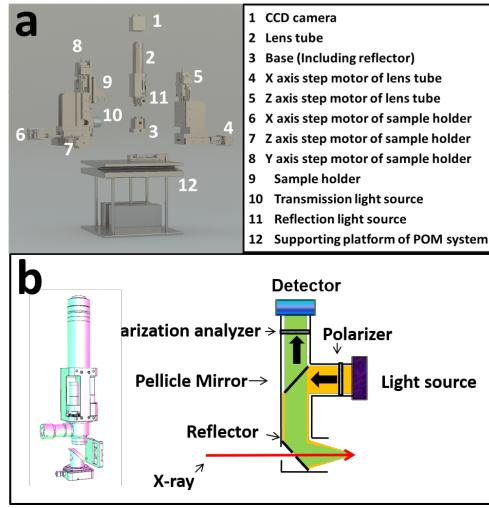


**Fig. 3.** POM overall disassembly and lens cone disassembly.

**Table 1.** Parameters of several common single lens

Radius $R/\mu\text{m}$	Aperture $2R_0/\mu\text{m}$	Area $\pi R_0^2/\text{mm}^{-2}$
200	881	0.609
100	623	0.305
50	440	0.152

60 First, CRL with a radius of  $50 \mu\text{m}$  is selected to calculate the relevant parameters.

61 Transmittance refers to the ratio of the light intensity after passing through the lens and the light intensity  
62 without passing through the lens. It can be calculated by Eq. 1[2]:

$$T_p = \frac{\int_0^{2\pi} d\theta \int_0^{R_0} e^{-\mu ND(r)} r dr}{\int_0^{2\pi} d\theta \int_0^{R_0} r dr} = \frac{1 - e^{-a}}{a} e^{-\mu Nd} \quad (1)$$

63 In Eq. 1,  $a = \mu NR_0^2/R$ ,  $R$  and  $R_0$  are given in Table 1,  $N$  is the number of lens,  $d$  is the minimum thickness  
64 of a single mirror. For parabolic lenses,  $d$  can be calculated with the following equation:

$$D(r) = d + 2 \times \frac{r^2}{2R} \quad (2)$$

65 The maximum processing thickness  $D(r)$  of the CRL selected in this experiment is 2 mm. Substituting  $D(r)$   
66 and  $r = R_0$  into the Eq. 2, the minimum  $d$  equals 1.032 mm.

67 According to the actual situation of beamline station shed size and pipeline layout, the image distance  
68 is about 400 mm and so is the focal length. The focal length calculation formula under the approximate  
69 condition of thin lens is :

$$f = R/2N\delta \quad (3)$$

70  $N$  is number of lenses,  $\delta$  is real part of refractive index to 1 offset.  $\delta$  can be calculated by following  
71 equation[3]:

$$\delta = \frac{2\pi\rho r_o}{k^2} \quad (4)$$

72  $\rho$  is electron number density,  $r_o$  is the electronic classical radius. For beryllium in 12KeV,  $\delta$  is  $2.36393 \times$   
73  $10^{-6}$ . When  $N$  is set to 30, the focal length is 352.5mm. This value meets the requirements described above.

74 Substituting  $N = 30$  and  $d = 1.032$  into the Eq. 1,  $T_p$  equals 0.327.

75 The flux of photons after passing through the lenses can be calculated by the following equation:

$$I = i \times T_p \times R \quad (5)$$

76  $i$  is the flux of incident X-ray. In BL19U2, under 220 mA current intensity,  $i = 2.5 \times 10^{12}$  photons/s,  $R$  is  
77 defined as the photon acceptance rate and equals 0.0598. Substituting these values into the Eq. 5,  $I$  equals  
78  $4.89 \times 10^{10}$  photons/s. This value is enough to study the structure of crystalline polymers.

79 For lens with a radius of  $100\mu\text{m}$  and  $200\mu\text{m}$ , after the same calculation,  $N$  is 60 and 120. Although  
80 a lens with a larger radius of curvature can be used to obtain a slightly larger flux, the number of lenses  
81 required is greatly increased. Comprehensive consideration, using 30 lenses with a radius of  $50 \mu\text{m}$  is the  
82 best choice.

83    **2.1.2 Reduce beam jitter**

84    Due to the thermal load caused by the high-power beam to the monochromator crystal and the vibration of  
85    the monochromator crystal caused by the liquid nitrogen cooling system of the monochromator, the current  
86    spot of the BL19U2 is jittered by about 10%, which will affect the strength stability of X-ray micro beam.

87       A processing software is compiled which integrates light intensity position data collection, data process-  
88       ing (calculation of beam center), data smoothing and filtering, PID control algorithm and control interface.  
89       Advanced FPGA technology is applied to design and implement a fuzzy adaptive PID controller. Beam  
90       position which is collected by the PID control loop in real time is compared with the set value. Then the  
91       comparison error is sent to the PID controller to calculate the control value through the PID control algo-  
92       rithm. Subsequently, the comparison error is input to the actuator of the monochromator pizeo to adjust  
93       the pizeo angle of the second crystal in real time, realize the constant feedback system of the beam center  
94       position and the constant light intensity feedback system. Finally, it is realized that the closed-loop control  
95       of the beam position and suppress low the beam drift of the frequency band to realize the stabilization of the  
96       BL19U2. Thus, the impact of beam jitter on the intensity of the focused beam is reduced.

97    **2.2 Construction of the combined system**

98       [Fig. 1](#) is the schematic diagram of the structure of synchrotron radiation X-ray micro-focusing polarized  
99       microscopy system. The combined system includes a micro-focusing component and an in situ polarized  
100      light microscope system. After the incident X-ray is focused by the CRL, it will pass through the light hole  
101      on the lower side of the POM and the sample, then the scattered signal will be received by the detector. The  
102      on-site construction diagram of the system is shown in [Fig. 4](#).

103       As shown in [Fig. 1](#), the CRL is mounted on a motorized platform. Including three-dimensional transla-  
104       tional electric platform (x, y, z three directions), one-dimensional swing stage (P angle) and one-dimensional  
105       rotating platform (R angle). The posture of CRL can be adjusted in five spatial dimensions.

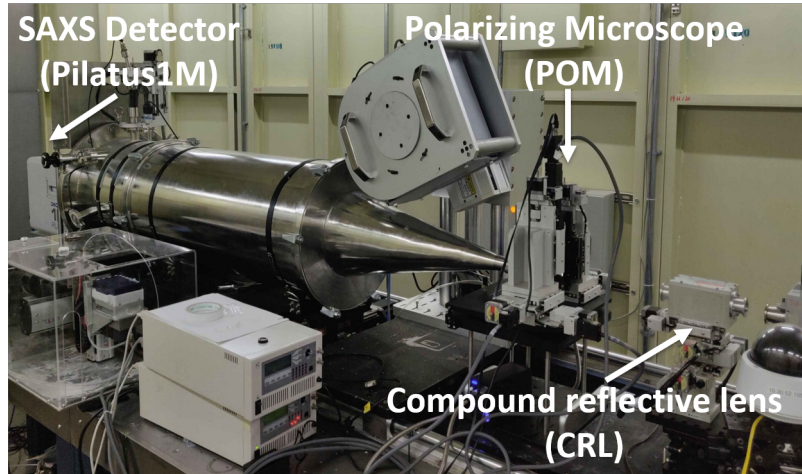


**Fig. 4.** Site map of the combined system.

106      The structure of POM used in the system is shown in [Fig. 3](#). As shown in [Fig. 3b](#), the optical system of  
 107     POM mainly consists of the following parts: a polarizer and analyzer that use ordinary white light sources  
 108     to generate polarized light; a half mirror located in the middle of the lens barrel; A flat mirror located at  
 109     the bottom of the lens barrel. The detector at the top is used to collect images. In this system, the detector  
 110     selects a Charge-coupled device(CCD) camera.

111      As shown in [Fig. 3a](#), the in situ POM system is also installed on a motorized support platform. A  
 112     stepping motor (4~5) installed on the side of the lens body realizes the translational adjustment of the lens  
 113     barrel in two dimensions. Similarly, the stepping motor (6~8) on the side of the sample holder realizes  
 114     its translational adjustment in three dimensions. The supporting platform (12) can be further divided into  
 115     three layers: the uppermost layer is a one-dimensional swing stage and a rotating table, the middle layer is  
 116     a two-dimensional (horizontal) translational electric platform, and the lowest layer is a three-dimensional  
 117     translational electric platform. Through the adjustment devices in all the above dimensions, The five spatial  
 118     dimensions of the entire optical system can be adjusted.

<sup>119</sup> **2.3 Determination of spot parameters**

<sup>120</sup> Once the combined system is installed in beamline, the beam can be adjusted. The main purpose of beam  
<sup>121</sup> adjustment is threefold: first, to ensure the connectivity of the integrated optical path, to ensure that X-rays  
<sup>122</sup> can pass through the system correctly. A series of elements on the fixed light path of the beamline are used to  
<sup>123</sup> adjust the primary light spot, and then the light path is adjusted using the POM and CRL spatial dimensions.  
<sup>124</sup> The current value of the ionization chamber can determine whether there is enough X-ray flux to irradiate  
<sup>125</sup> the sample. The second purpose is to verify whether the CRL is accepted to focus the primary spot to a  
<sup>126</sup> sufficiently small spot size. Only when the size is basically in line with the theoretical value to achieve  
<sup>127</sup> a sufficiently small spatial resolution, can the microstructure of the research system be characterized; the  
<sup>128</sup> third is to adjust the position of the light spot to the center of the field of view, while adjusting the angle  
<sup>129</sup> of the plane mirror to make the polarized light that reaches the sample after being reflected twice by  
<sup>130</sup> the half mirror and the plane mirror is focused on the X-ray at this point in the sample. The detection point  
<sup>131</sup> of the sample is located in the center of the field of view, and the detection position will not shift even if  
<sup>132</sup> the magnification of the polarizing microscope is changed. In order to achieve the latter two purposes, we  
<sup>133</sup> need to observe the spot in real time under POM. For this reason, we install a cesium iodide crystal on the  
<sup>134</sup> sample stage. Cesium iodide crystal has the characteristic of emitting fluorescence under X-rays, so it is also  
<sup>135</sup> called scintillation crystal. In this system, the X-ray spot position is calibrated by the fluorescence spectrum  
<sup>136</sup> generated by cesium iodide under POM.

<sup>137</sup> The step motors used in this system are all produced by Kohzu Corporation. The positioning accuracy  
<sup>138</sup> can reach 1um, which is enough for precise spatial position adjustment. Adjust the CRL posture so that the  
<sup>139</sup> incident X-ray can pass through the lenses correctly and be focused. Then adjust the y-direction motor of  
<sup>140</sup> the POM sample stage, so that the scintillation crystal is correctly focused and imaged in the field of view of  
<sup>141</sup> the polarizing microscope. Finally, adjust the x and z direction motors to move the center of the field of view  
<sup>142</sup> to the fluorescent spot. In the PC imaging software, a cross ruler will be displayed to assist in positioning.

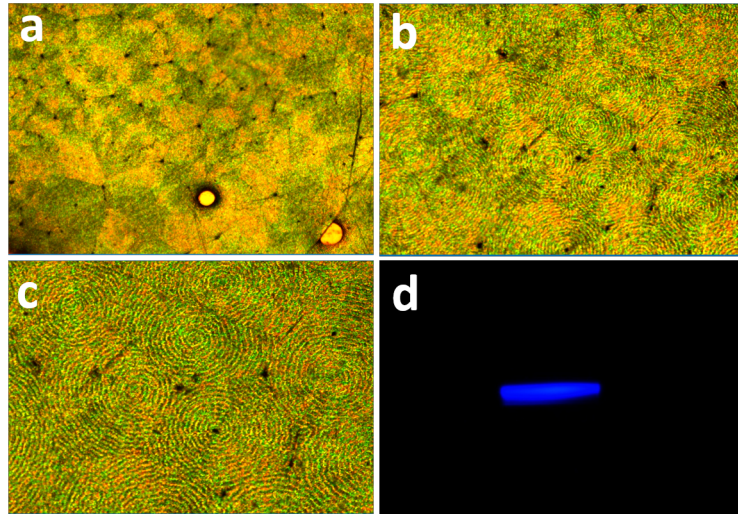


**Fig. 5.** Result of commissioning POM on site

143 The theoretical focus size of the focus spot is about 5um 5um. In order to verify the difference between  
 144 the actual adjustment and the theoretical calculation, two methods are usually used. As shown in Figures 6a  
 145 and 6b, the first is to visually observe through imaging software and use a ruler to make rough measurements.  
 146 This method is relatively intuitive and fast, but the accuracy is insufficient. The second method is to use  
 147 ionization chamber current data for fitting. According to related theories, FWHM of the first derivative of  
 148 ionization chamber current to displacement can refer to the spot size. The representative fitting results of this  
 149 system are shown in Fig. 6c, As shown in Fig. 6d, Gaussian fitting is performed on the original curve, and  
 150 the FWHM of the fitted peak is calculated to be  $5.43\mu\text{m} \times 6.52\mu\text{m}$ . This value can represent the effective  
 151 size of the light spot, and this value basically achieves the expected effect.

#### 152 **2.4 Collection of micro-focus X-ray scattering data**

153 After adjusting the size and position of the light spot, it can be used to characterize the micro-domain struc-  
 154 ture of related polymer crystals. First, determine the position that needs to be characterized under the POM,

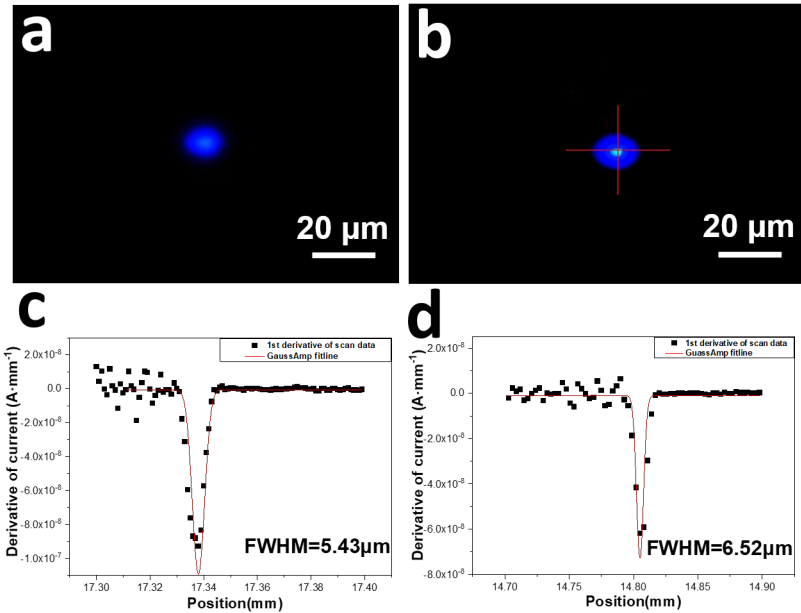


**Fig. 6.** Result of CRL micro-focus (facula and flux)

and then use the motor installed on the platform to remove the visible light source. Pass in synchrotron X-rays to collect scattered signals. At the SSRF-BL19U2 line station, X-rays with an energy of 12keV are often used, and the distance between the sample and the detector is 2700mm. The scattering signal is collected by Pilatus1M detector (981\*1043pixel, with a pixel size of 172um\*172um).

### 3 Application

In order to verify the feasibility of the entire combined system, the spherulites with annulus and fibers with a sheath-core structure are used as research examples. Micro-focused X-ray spot is used for micro-area resolution, and the scattering information of small structures that cannot be obtained by ordinary small-angle scattering experiments can be obtained.

<sup>164</sup> **3.1 Microstructure of ringed spherulites**

<sup>165</sup> Spherulites are the most common morphological structure of polymer materials, and they also play a vital  
<sup>166</sup> role in the physical, chemical and mechanical properties of polymer materials. Its multi-level structure is  
<sup>167</sup> complicated, and many basic scientific issues related to its structure need to be further explored. At present,  
<sup>168</sup> in the study of the microstructure of zonal spherulites, there are several scientific problems that need to be  
<sup>169</sup> explained urgently. The first problem is the correlation between the growth axis of the polymer ring-belt  
<sup>170</sup> spherulites and the torsion chirality of the lamellae. One theory is that the growth axis affects the chirality  
<sup>171</sup> of the lamella torsion by changing the pressure distribution on the lamella plane. micro-focus X-ray can be  
<sup>172</sup> used to determine the growth axis of each region and the tilt torsion behavior of the mapping crystal plane  
<sup>173</sup> along the growth axis, revealing the correlation between the crystal growth axis and the lamella torsion  
<sup>174</sup> chirality. It can provide a scientific basis for clarifying the transfer behavior of chirality between the multi-  
<sup>175</sup> level structure of polymer spherulites. The second problem is the cross-nucleation of polymer spherulites  
<sup>176</sup> during the crystallization. Through micro-focus X-ray, the crystalline transformation information at the front  
<sup>177</sup> of spherulite growth are monitored in situ, including crystal plane, orientation, whether there is a transition  
<sup>178</sup> (gradient) zone to reveal the cross-nucleation mechanism in polymer crystals, and clarify multiple crystal  
<sup>179</sup> types the correlation and the similarities and differences between polymer cross nucleation and traditional  
<sup>180</sup> cross nucleation of small molecule.

<sup>181</sup> We chose banded spherulites as a sample to verify the usability of the micro-focusing polarizing micro-  
<sup>182</sup> scope system. Microbeam X-ray scans are especially informative.

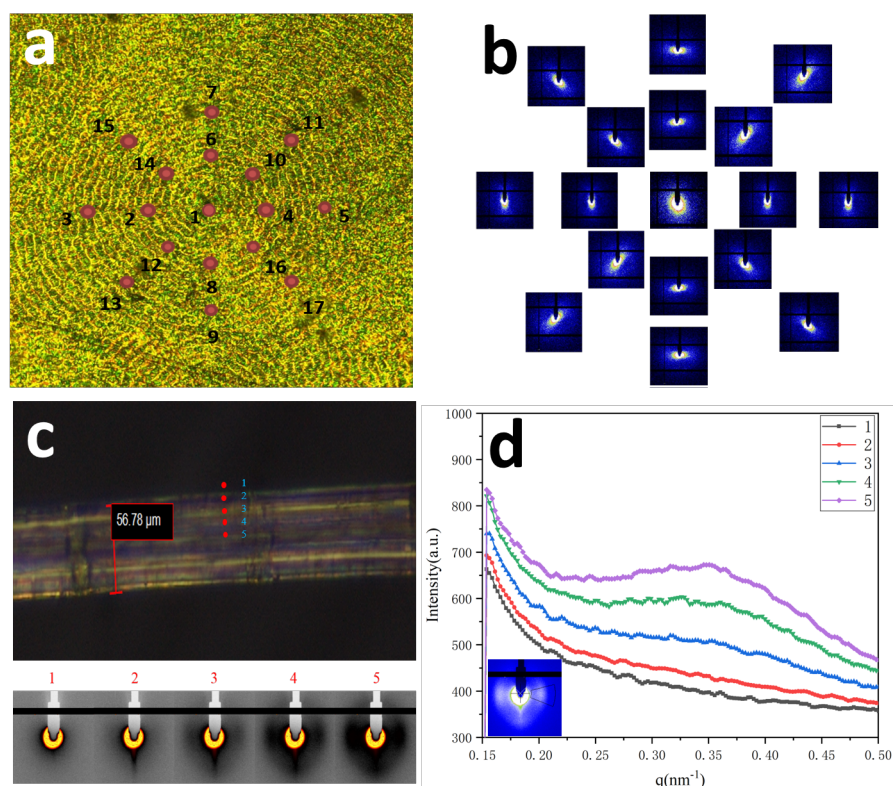


**Fig. 7.** The application sample of the system

<sup>183</sup> **3.2 The skin and core structure of the fiber**

<sup>184</sup> **4 Conclusion**

<sup>185</sup> **References**

- <sup>186</sup> [1] Jun Xu, S. Z., Haimu Ye & Guo, B. Organization of twisting lamellar crystals in birefringent banded  
<sup>187</sup> polymer spherulites: A mini-review. *Crystals* **7** (2017).
- <sup>188</sup> [2] Lengeler, B. *et al.* Imaging by parabolic refractive lenses in the hard X-ray range. *Journal of Synchrotron  
189 Radiation* **6**, 1153–1167 (1999). URL <https://doi.org/10.1107/S0909049599009747>.
- <sup>190</sup> [3] Als-Nielsen, J. & McMorrow, D. *Elements of Modern X-ray Physics* (Wiley, 2011). URL <https://books.google.co.jp/books?id=rlqlbowlTRMC>.